

# Switching through symmetry breaking in coupled nonlinear micro-cavities

**Björn Maes, Marin Soljačić, John D. Joannopoulos**

*Dept. of Physics, Center for Materials Science and Engineering, Research Laboratory of  
Electronics, Massachusetts Institute of Technology,  
77 Massachusetts Avenue, Cambridge 02139, Massachusetts, USA  
[bjorn.maes@ugent.be](mailto:bjorn.maes@ugent.be)*

**Peter Bienstman, Roel Baets**

*Photonics Research Group, Ghent University,  
St.-Pietersnieuwstraat 41, 9000 Ghent, Belgium*

**Simon-Pierre Gorza, Marc Haelterman**

*Service d'Optique et Acoustique, Université Libre de Bruxelles,  
Avenue F.D. Roosevelt 50, 1050 Brussels, Belgium*

**Abstract:** We describe stable symmetry-breaking states in systems with two coupled nonlinear cavities, using coupled-mode theory and rigorous simulations. Above a threshold input level the symmetric state of the passive Kerr system becomes unstable, and we show how this phenomenon can be employed for switching and flip-flop purposes, using *positive* pulses only. A device with compact photonic crystal microcavities is proposed by which we numerically demonstrate the principle.

© 2006 Optical Society of America

**OCIS codes:** (190.1450) Bistability; (230.4320) Nonlinear optical devices.

---

## References and links

1. T. Yabuzaki, T. Okamoto, M. Kitano, and T. Ogawa, "Optical bistability with symmetry-breaking," *Phys. Rev. A* **29**, 1964–1972 (1984).
2. K. Otsuka and K. Ikeda, "Hierarchical multistability and cooperative flip-flop operation in a bistable optical system with distributed nonlinear elements," *Opt. Lett.* **12**, 599–601 (1987).
3. K. Otsuka, "All-optical flip-flop operations in a coupled element bistable device," *Electron. Lett.* **24**, 800–801 (1988).
4. K. Otsuka, "Pitchfork bifurcation and all-optical digital signal-processing with a coupled-element bistable system," *Opt. Lett.* **14**, 72–74 (1989).
5. M. Haelterman and P. Mandel, "Pitchfork bifurcation using a 2-beam nonlinear fabry-perot-interferometer - an analytical study," *Opt. Lett.* **15**, 1412–1414 (1990).
6. T. Peschel, U. Peschel, and F. Lederer, "Bistability and symmetry-breaking in distributed coupling of counter-propagating beams into nonlinear wave-guides," *Phys. Rev. A* **50**, 5153–5163 (1994).
7. I.V. Babushkin, Y.A. Logvin, and N.A. Loïko, "Symmetry breaking in optical dynamics of two bistable thin films," *Quantum Electron.* **28**, 104–107 (1998).
8. J.P. Torres, J. Boyce, and R.Y. Chiao, "Bilateral symmetry breaking in a nonlinear Fabry-Perot cavity exhibiting optical tristability," *Phys. Rev. Lett.* **83**, 4293–4296 (1999).
9. L. Longchambon, N. Treps, T. Coudreau, J. Laurat, and C. Fabre, "Experimental evidence of spontaneous symmetry breaking in intracavity type II second-harmonic generation with triple resonance," *Opt. Lett.* **30**, 284–286 (2005).
10. M. Soljačić, M. Ibanescu, S.G. Johnson, Y. Fink, and J.D. Joannopoulos, "Optimal bistable switching in nonlinear photonic crystals," *Phys. Rev. E* **66**, 055601(R) (2002).
11. S.F. Mingaleev and Y.S. Kivshar, "Nonlinear transmission and light localization in photonic-crystal waveguides," *J. Opt. Soc. Am. B* **19**, 2241–2249 (2002).

12. M. Notomi, A. Shinya, S. Mitsugi, G. Kira, E. Kuramochi, and T. Tanabe, "Optical bistable switching action of Si high-Q photonic-crystal nanocavities," *Opt. Express* **13**, 2678–2687 (2005), <http://www.opticsinfobase.org/abstract.cfm?URI=oe-13-7-2678>.
  13. P.E. Barclay, K. Srinivasan, and O. Painter, "Nonlinear response of silicon photonic crystal microresonators excited via an integrated waveguide and fiber taper," *Opt. Express* **13**, 801–820 (2005), <http://www.opticsinfobase.org/abstract.cfm?URI=oe-13-3-801>.
  14. B. Maes, P. Bienstman, and R. Baets, "Switching in coupled nonlinear photonic-crystal resonators," *J. Opt. Soc. Am. B* **22**, 1778–1784 (2005).
  15. P. Bienstman and R. Baets, "Optical modelling of photonic crystals and VCSELs using eigenmode expansion and perfectly matched layers," *Opt. Quantum Electron.* **33**, 327–341 (2001).
  16. B. Maes, P. Bienstman, and R. Baets, "Modeling of Kerr nonlinear photonic components with mode expansion," *Opt. Quantum Electron.* **36**, 15–24 (2004).
  17. M.F. Yanik, S. Fan, and M. Soljačić, "High-contrast all-optical bistable switching in photonic crystal microcavities," *Appl. Phys. Lett.* **83**, 2739–2741 (2003).
  18. P.V. Paulau and N.A. Loïko, "Self-sustained pulsations of light in a nonlinear thin-film system," *Phys. Rev. A* **72**, 013819 (2005).
  19. M. Soljačić and J.D. Joannopoulos, "Enhancement of nonlinear effects using photonic crystals," *Nature Materials* **3**, 211–219 (2004).
  20. Z. Wang and S. Fan, "Optical circulators in two-dimensional magneto-optical photonic crystals," *Opt. Lett.* **30**, 1989–1991 (2005).
- 

## 1. Introduction

Symmetry-breaking is at the heart of many physical phenomena. Here, we describe the breaking of left-right symmetry in a nonlinear optical system. In linear symmetric systems the breaking is absent, as superposition of equal inputs from left and right results in equal outputs to the left and right. Here, as usual, the symmetry breakup arises from coupling and feedback between two nonlinearly adjustable modes. In the linear case both modes are excited with the same strength. In the nonlinear case this excitation shifts the resonance frequencies of the modes. Because of the coupling of intensities between the modes, it is possible that the symmetric situation is no longer stable at a certain input power. Then the system will drift to a situation where one mode is more excited than the other, and thus an asymmetric state arises.

Different nonlinearities can instigate the breaking, but we employ the instantaneous Kerr nonlinearity, where the index depends on the intensity of the local field. Previous optical settings in which the pitchfork bifurcation has been explored [1-9] include a Fabry-Pérot cavity with two inputs at an angle [5]. In [7] two coupled cavities are studied, but the nonlinearity stems from two-level atoms. Here, in contrast, we study passive cavities.

The principle can be applied to many different systems in which nonlinear coupled cavities are present. As a possible realistic implementation we study photonic crystal (PhC) defects. These structures possess practically achievable nonlinear effects such as bistability through a folding bifurcation [10, 11], which was recently demonstrated experimentally [12, 13]. Here we extend the switching capabilities by adding another cavity and using inputs from both sides. We show that this system presents a pitchfork bifurcation, that can be flipped with the use of both positive (an increase in intensity) and negative (a dip in intensity) pulses. For certain applications it is much easier to switch with positive pulses only. By use of coupled-mode theory (CMT) we give a precise and simple analytical description of the processes, that agrees well with simulations.

## 2. Analytical description

The structure, see Fig. 1(a), is described by [14]:

$$\frac{da_j}{dt} = \left[ i(\omega_0 + \delta\omega_j) - \frac{1}{\tau} \right] a_j + df_j + db_{j+1}, \quad (1)$$

$$b_j = \exp(i\phi)f_j + da_j, \quad (2)$$

$$f_{j+1} = \exp(i\phi)b_{j+1} + da_j, \quad (3)$$

for  $j = 1, 2$ . Here  $d = i\exp(i\phi/2)/\sqrt{\tau}$ , where  $\phi$  represents the phase that depends on the waveguide length and the PhC reflection properties. The nonlinear frequency shift is  $\delta\omega_j = -|a_j|^2/(P_0\tau^2)$ , with  $P_0$  the ‘characteristic nonlinear power’ of the cavity [10]. In these equations  $|a_j|^2$  is the energy in the cavity mode.  $|f_j|^2$  (resp.  $|b_j|^2$ ) represents the power flowing in the (single-mode) waveguide in the forward (resp. backward) direction. Thus,  $|f_1|^2 \equiv P_{in}^L$  (resp.  $|b_3|^2 \equiv P_{in}^R$ ) is the input power from the left (resp. right), and  $|b_1|^2 \equiv P_{out}^L$  (resp.  $|f_3|^2 \equiv P_{out}^R$ ) is the output power to the left (resp. right).

In the following we show that asymmetric solutions can exist, *even if the system is excited with equal powers from both sides*. The analysis is analogous to the one in [5]. We work in the frequency domain, so  $d/dt$  becomes  $i\omega$ . Eliminating  $f_2$  and  $b_2$  we obtain:

$$\left[ i(\omega_0 - \omega + \delta\omega_1) - \frac{1}{\tau} \right] a_1 + \kappa(\gamma a_1 + a_2) = -df_1, \quad (4)$$

$$\left[ i(\omega_0 - \omega + \delta\omega_2) - \frac{1}{\tau} \right] a_2 + \kappa(\gamma a_2 + a_1) = -db_3, \quad (5)$$

with  $\gamma = \exp(i\phi)$  and  $\kappa = d^2/(1 - \gamma^2)$ . We equate the left sides of Eqs. 4 and 5, as we assume  $f_1 = b_3$ , thus equal input power (and phase) from both sides. We take the modulus squared, and after factoring we get:

$$(A - B) [(A^2 + AB + B^2) + 2\Delta'(A + B) + \Delta'^2 + 1/4] = 0, \quad (6)$$

with dimensionless cavity energies  $A = \alpha|a_1|^2$  and  $B = \alpha|a_2|^2$ , where  $\alpha = -1/(P_0\tau)$ . Furthermore, the detuning  $\Delta' = \Delta + \tan(\phi/2)/2$ , with  $\Delta = \tau(\omega_0 - \omega)$ . From Eq. 6 we learn that there is

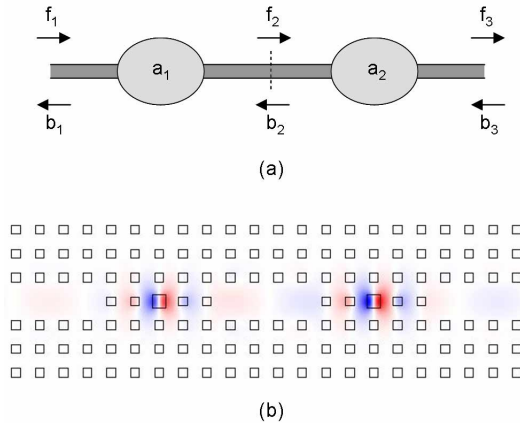


Fig. 1. (a) Schematic of the coupled cavity structure. (b) The PhC device, with 4 periods in between the switches. An electric field distribution is superimposed to illustrate the defect modes.

the possibility of an asymmetric solution  $A \neq B$ , apart from the symmetric solution  $A = B$ . The asymmetric solution appears (for certain input powers) if the detuning  $\Delta'$  is chosen correctly, and if the solution is stable.

We now derive a criterion for  $\Delta'$  concerning the existence of the symmetry-breaking solution. The factor for the asymmetric solution (between square brackets in Eq. 6) can be seen as a quadratic equation in  $B$ . For the existence of real solutions its discriminant has to be positive:  $-3A^2 - 4\Delta'A - 1 > 0$ . It is positive if  $A$  lies between the values  $(-2\Delta' \pm \sqrt{4\Delta'^2 - 3})/3$ . Thus the asymmetric solution exists if  $|\Delta'| > \sqrt{3}/2$ . For positive nonlinearity ( $\alpha < 0$ ) one needs  $A < 0$  and thus  $\Delta' > 0$ , so one takes  $\Delta' > \sqrt{3}/2$ , and vice versa for negative nonlinearity.

Two examples of the input-output curves are shown in Fig. 2. We depict the powers instead of the mode amplitudes, as derived from Eqs. 4 and 5. Note that these curves depend both on  $\Delta$  and  $\phi$ , instead of only on  $\Delta'$ . Calculations of Eqs. 4 and 5 proof this (not shown). Above a certain input power level the symmetric solution becomes unstable, and the system switches to an asymmetric state. Linear stability analysis shows indeed that the symmetric solution destabilizes, if an asymmetric solution exists. More power exits to the left than to the right, or vice versa. It is possible to obtain high contrasts between the left and right output powers; even a zero output in one direction is attainable. At high detuning the shape of the curve becomes more complex, and the asymmetric branch shows multistability, see Fig. 2(b).

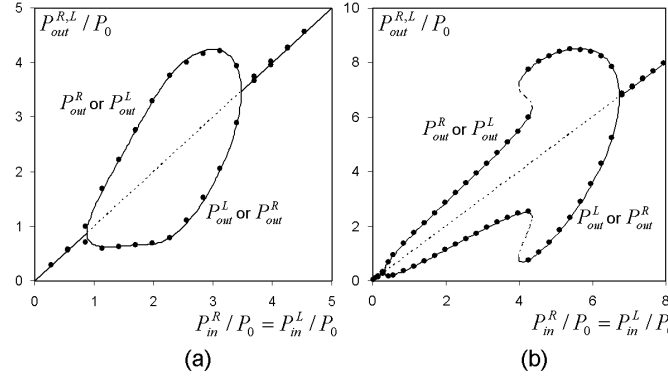


Fig. 2. Output power versus input power for (a)  $\Delta = 1.039$ ,  $\phi = 0.570$  and (b)  $\Delta = 2.0$ ,  $\phi = 0.595$ . Stable and unstable states are shown with solid and dashed lines, respectively. Dots show rigorous simulation results.

### 3. Numerical modeling

As a model system for rigorous simulations we use the 2D PhC structure depicted in Fig. 1(b). We use a square lattice with period  $a$  of squares with side length  $0.4a$  and index 3.5 in air. The two identical defect rods have side  $0.6a$ . The nonlinear material has a realistic nonlinear coefficient  $n_2 = 2.15 \times 10^{-17} \text{m}^2/\text{W}$ . We use TM-polarization (one E-field component out-of-plane).

From linear calculations with the mode-expansion technique [15], which computes exact solutions of the vectorial Maxwell equations, we obtain that  $\omega_0 = 0.321169(2\pi c/a)$  and  $1/\tau = 1.623 \times 10^{-4}(2\pi c/a)$ , thus  $Q = \omega_0\tau/2 = 990$ . By changing the intermediate waveguide length the phase  $\phi$  can be varied. We used eight periods between the cavities (thus four more than depicted in Fig. 1(b)); in that case the phase can be linearly approximated by  $\phi = -163.9\omega/(2\pi c/a) + 2.9$ .

For precise nonlinear calculations we use an iterative extension of the mode-expansion method, that uses a grid for the nonlinear sections [16]. The method allows to study the stable states in the frequency domain. Only the large defect rods are considered nonlinear, with a  $12 \times 8$ -grid. Using the *horizontal* symmetry plane only one upper half in Fig. 1 needs to be simulated. Furthermore, the linear sections have to be calculated once during iteration at a fixed frequency. The use of 60 eigenmodes is sufficient to obtain converged results. From single switch nonlinear calculations we get  $P_0 = 3.52\text{MW/m}$ . CMT with these parameters and the rigorous calculations with two switches agree very well, as can be seen in Fig. 2. Note that  $P_0$  is proportional to  $1/Q^2$  [10], therefore high  $Q$  factors give rise to practical switching powers, as already obtained in slab structures [12, 13].

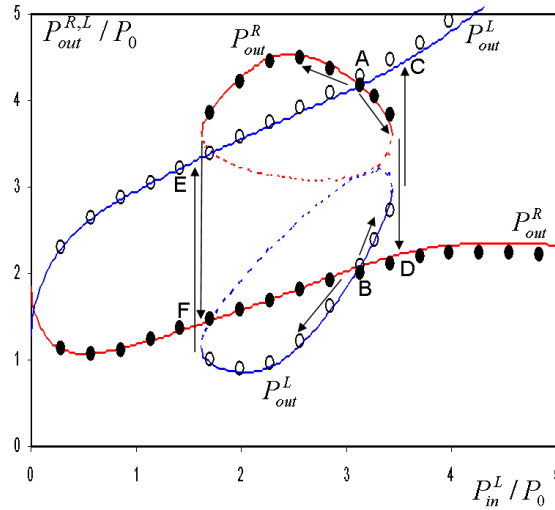


Fig. 3. Output powers versus left input power  $P_{in}^L$  at  $\Delta = 1.039$ ,  $\phi = 0.570$  and  $P_{in}^R = 3.125P_0$ . Stable states for  $P_{out}^R$  (resp.  $P_{out}^L$ ) are shown with red (resp. blue) solid lines. Dashed lines indicate unstable states. Dots (resp. circles) show rigorous simulation results for  $P_{out}^R$  (resp.  $P_{out}^L$ ). Labels AB, CD and EF display key states.

#### 4. Switching

The system can be switched from one asymmetric state to the other by adding a positive or negative pulse to the side with lower output power. The switching mechanism becomes clear from Fig. 3. Here the input power from the right  $P_{in}^R$  is held constant, while the one from the left  $P_{in}^L$  is varied. Starting from state AB, in the situation where  $P_{out}^R > P_{out}^L$ , we follow the arrows to the right, if we increase  $P_{in}^L$ . Eventually this branch stops and we flip to state CD, with  $P_{out}^R < P_{out}^L$ . Decreasing  $P_{in}^L$  we again reach state AB, but now the outputs are flipped. We could also follow the arrows to the left, by decreasing  $P_{in}^L$ , starting from state AB, again with  $P_{out}^R > P_{out}^L$ . Then we reach the left end of the branch, and the solution jumps to the state EF, with  $P_{out}^R < P_{out}^L$ . Increasing  $P_{in}^L$  brings the system to the flipped state AB. Once the system is flipped, one needs to add or remove power at the other side to flip again. This corresponds to changing the left/right labels L and R in Fig. 3.

To ascertain that switching is possible by positive pulses we have performed time-domain simulations of the CMT equations. It was previously shown that these equations provide a highly accurate picture of temporal switching aspects [17]. An example of a state flip is shown

in Fig. 4. The same parameters are used as in Fig. 3. At times  $< 0$  all input powers are considered zero. In the beginning after time zero a slight perturbation of  $P_{in}^R$  brings the system into state AB with  $P_{out}^R > P_{out}^L$ . Then at a time  $4 \times 10^4$  periods  $P_{in}^L$  is increased to  $3.7P_0$ , that is able to switch the system into state CD, in agreement with Fig. 3. After a time  $9 \times 10^4$  periods we equalize the input powers again,  $P_{in}^L = P_{in}^R = 3.125P_0$ , and we obtain the flipped AB state. Other switching aspects, such as flipping with negative pulses and being unable to switch with weak pulses, have also been checked.

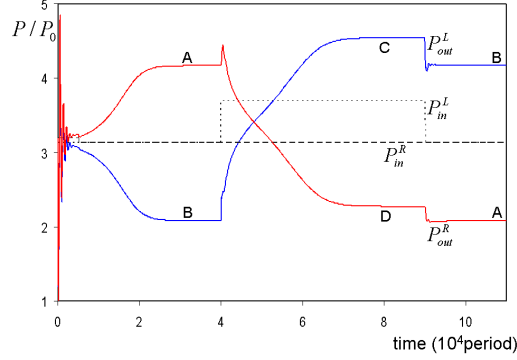


Fig. 4. Switching of the state by adding power to the left input  $P_{in}^L$ . Here  $\Delta = 1.039$ ,  $\phi = 0.570$  and the period is  $2\pi/\omega$ . After an initial small perturbation of the right input power it is held constant at  $P_{in}^R = 3.125P_0$ . The dotted (dashed) line shows  $P_{in}^L$  ( $P_{in}^R$ ). The blue and red lines depict  $P_{out}^L$  and  $P_{out}^R$ , respectively.

In experiments the cavities are not identical. We have checked the case where the resonance frequencies differ, say one has  $\omega_0^A$  and  $\omega_0^B$ . The solutions are more complex (the states become non-degenerate). However, the functionality remains the same, up until a certain resonance frequency difference. This tolerance depends upon the detuning. With the parameters of Fig. 2(b), a non-optimized value for the tolerance amounts to  $|\omega_0^A - \omega_0^B|/\omega_{avg} < 0.5/Q$ , with  $\omega_{avg} = (\omega_0^A + \omega_0^B)/2$ .

In order to separate the counter-propagating beams in the ports one could use a photonic crystal circulator [20], or adjust the design. Note that the related system with two-level atoms in thin coupled films presents a rich time-domain behavior, such as self-sustained pulsations [18]. Therefore, analogous phenomena may be observable in the structure considered here. Furthermore, many PhC-geometries have been studied thus far [19]. It is expected that the study of these elements will reveal other asymmetric states.

## 5. Conclusion

In conclusion, we study a new switching scheme involving symmetry breaking states in coupled nonlinear cavities. CMT provides simple analytical insight and a good agreement with rigorous simulations is observed. The use of positive pulses for flip-flop operation is described by both frequency- and time-domain results. Symmetry breaking is a powerful principle in nature, and the presented behavior should be general for many types of nonlinearities and devices.

## Acknowledgments

BM and PB acknowledge postdoctoral fellowships from the Funds for Scientific Research - Flanders (FWO-Vlaanderen). We acknowledge the Belgian DWTC project IAP-Photon and the NSF MRSEC grant DMR-02-13282.